Pergamon

Continental Shelf Research, Vol. 16, No. 11, pp. 1437–1452, 1996

0278–4343/96 $15.00 + 0.00

0278–4343(95)00087–9

Three-dimensional island wakes in the field, laboratory experiments and numerical models

ERIC WOLANSKI,* TAKASHI ASAEDA,† AKIHIRO TANAKA† and ERIC DELEERSNIJDER‡

(*Received* 10 *July* 1995; *accepted* 3 *November* 1995)

Abstract—Results of field, laboratory and numerical studies are used to describe the three-dimensional circulation in a barotropic island wake in shallow waters. Bottom friction generates a closed circulation characterized by a strong upwelling (typically 10–20 m h^{-1}) in the bulk of the eddy and an even larger downwelling velocity in a narrow zone along the edges of the eddy. This downwelling exists at the solid boundaries of the island and also all along the separation streamline. This circulation can be realistically modeled numerically provided the intense turbulence in the free shear layers is explicitly parameterized. This secondary circulation aggregates buoyant material along the edges of the eddy even in well-mixed coastal waters. Copyright © 1996 Elsevier Science Ltd

INTRODUCTION

Flows past headlands, islands and coral reefs in shallow, well-mixed coastal waters are very complex. High values of the concentration of suspended sediment and plankton make apparent, in aerial or satellite pictures, complex surface features comprising eddies, jets and shear zones (Maxwell, 1968; Wolanski *et al.*, 1984a,b; Ingram and Chu, 1987; Pattiaratchi *et al.*, 1987; Wolanski, 1994). Detailed field observations of the circulation have relied either on a large number of moored current meters and radar-tracked drogues (Wolanski *et al.*, 1984a,b) or on ADCP data (Geyer and Signell, 1990; Geyer, 1993). Both methods have advantages and disadvantages. With the former method, a synoptic but low spatial resolution view of the current distribution is obtained throughout a tidal cycle. With the latter method, details of currents are available along ship tracks at the cost of losing synopticity.

Depth-averaged two-dimensional numerical models are known to yield eddies behind islands and headlands (Pingree and Maddock, 1979; Heathershaw and Hammond, 1980;

*Australian Institute of Marine Science, PMB No. 3, Townsville MC, Queensland 4810, Australia.
†Department of Environmental Science, Saitama University, 255 Shimo-Okubo, Urawa, Saitama 358, Japan.
‡G. Lemaitre Institute of Astronomy & Geophysics, Catholic University of Louvain, Chemin du Cyclotron 2, B-1348 Louvain-La-Neuve, Belgium, and Research Associate, National Fund for Scientific Research of Belgium.

Falconer *et al.*, 1986; Ingram and Chu, 1987; Signell and Geyer, 1991). These small-scale models turn out to be reliable when extensive field data are available for open boundary forcing and model verification in the simple situation where the dominant tidal currents simply reverse direction by 180° without rotating with the tides (Falconer *et al.*, 1986; Wolanski *et al.*, 1988). When the far-field currents are rotating with the tides, eddies can also form behind an island, but either they are periodically ejected with the tides (Hamner and Hauri, 1977) or they rotate around the island with the tidal currents (Wolanski *et al.*, 1989). Models are only able to reproduce qualitatively these latter observations, possibly because of ill-defined open boundary conditions (Oliver *et al.*, 1992).

Of great interest is the three-dimensional circulation in shallow waters. This circulation is made apparent by the aggregation of buoyant particles in downwelling zones in patches or in slick lines. Tidal mixing can generate density fronts near islands (Simpson *et al.*, 1982), and the resulting baroclinic currents lead to surface aggregation of plankton along the density fronts, a phenomenon reported over 40 years ago by Boden (1952) and for which numerous examples exist (Uda and Ishino, 1958; Wolanski and Hamner, 1988; Franks, 1992). Aggregation of floating material or upward-swimming organisms, such as coral eggs, plankton and fish larvae, is not confined to baroclinic situations; it also occurs in barotropic situations, in shallow, well-mixed waters near headlands and islands (Fig. 1a; see also Alldredge and Hamner, 1980; Hamner and Hauri, 1981; Wolanski and Hamner, 1988; Kingsford *et al.*, 1991; Wolanski, 1994). The aerial photographs of Ingram and Chu (1987), St. John and Fond (1992) and Wolanski (1993, 1994) also show aggregation of floating matter along separation streamlines.

The aggregation of biological material in turn influences the distribution of benthic assemblages and of pelagic secondary and tertiary predators, and essentially is akin to negative diffusion. The secondary, topographically induced circulation also finds geomorphic, navigation and engineering applications, since it controls the formation and movement of shoals and sand banks (Heathershaw and Hammond, 1980) and even the migration of river meanders (Kikkawa *et al.*, 1976).

Wolanski *et al.*, (1984a) proposed an analytical model of the flow in an eddy in shallow coastal waters. The flow is qualitatively similar to that in a tea cup, with convergent flow near the bottom due to rotation, upwelling in the center of the eddy and downwelling along the edge. Field observation of this secondary flow are few but show steering towards the eddy center of the near-bottom currents by as much as 10–15% of the surface current. (Deleersnijder *et al.*, 1992; Geyer, 1993). There are no previous measurements of the vertical flows in eddies in coastal waters.

Three-dimensional numerical model studies of an island wake (Deleersnijder *et al.*, 1992) were able to predict an upwelling at the center of the eddy and a downwelling at the solid boundaries of the island, but no downwelling was predicted at the fluid–fluid edges of the eddy.

The results of field, laboratory and three-dimensional numerical studies of island wakes are reported here. The laboratory studies confirm the existence of a strong secondary circulation. Upwelling occurs over the bulk of the eddy and downwelling is restricted to a narrow ring around the edges of the eddy. A three-dimensional numerical model is able to reproduce these observations for rotating flow in a closed, circular basin and for an island wake, provided the model includes the parameterization of the high vertical turbulence levels in the free shear layer representing the fluid–fluid edges of the eddy. Maximum vertical velocities of 0.01 m s^{-1} are predicted, in agreement with field observations. The

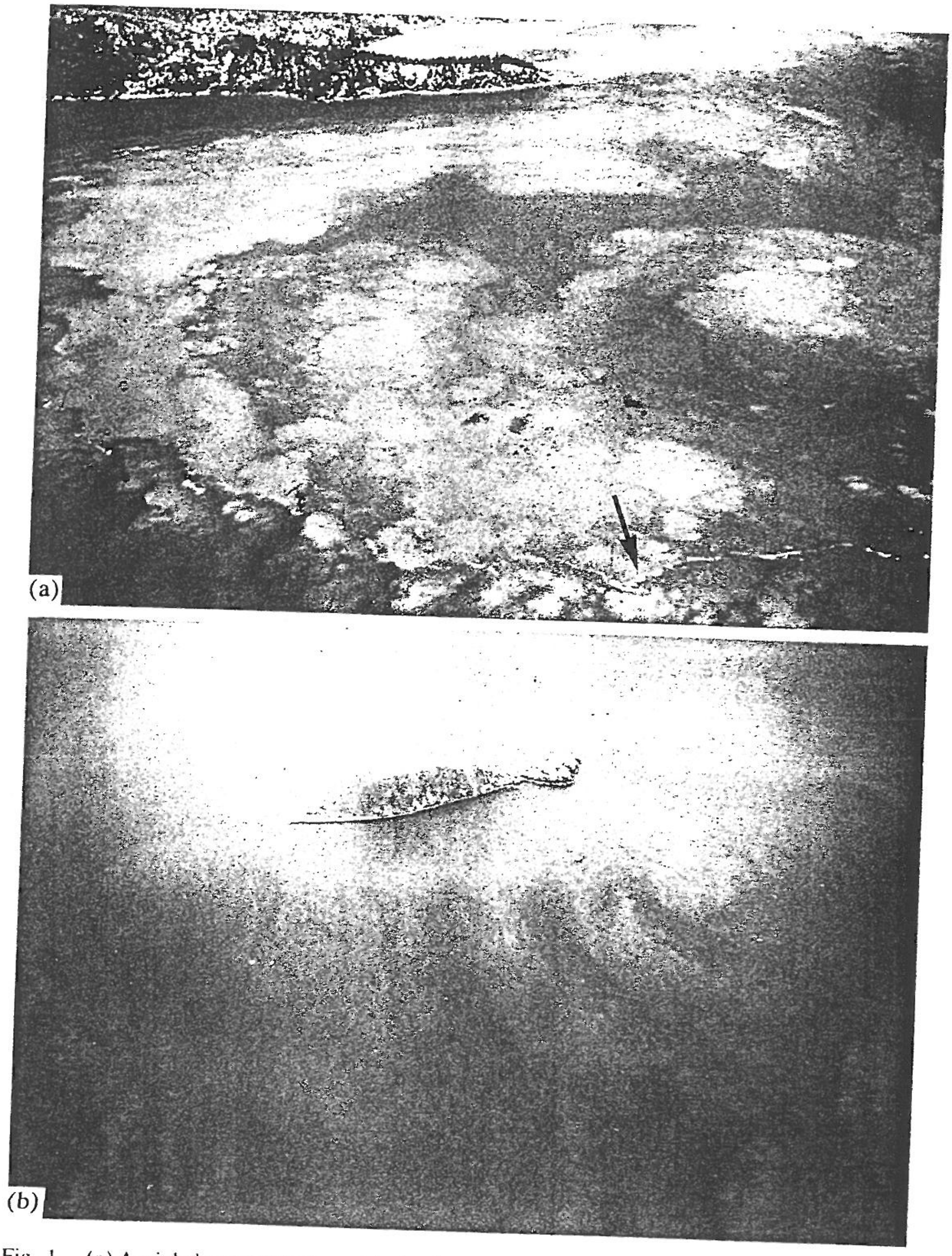

Fig. 1. (a) Aerial photograph of an eddy shed by a headland in shallow, well-mixed coastal waters in the Whitsundays Islands, Australia. The arrow points to a coral slick along the edge of the eddy. Aerial photographs of Rattray Island, Australia, (b) 2 h into the flood tide showing the spirals of muddy water emanating from the center of the eddy, and (overleaf) (c) the free shear layer downstream of the separation point 4 h into the flood tide when the wake was fully developed. (d) Oblique photograph of dyed streaklines at different depths in the laboratory experiment.

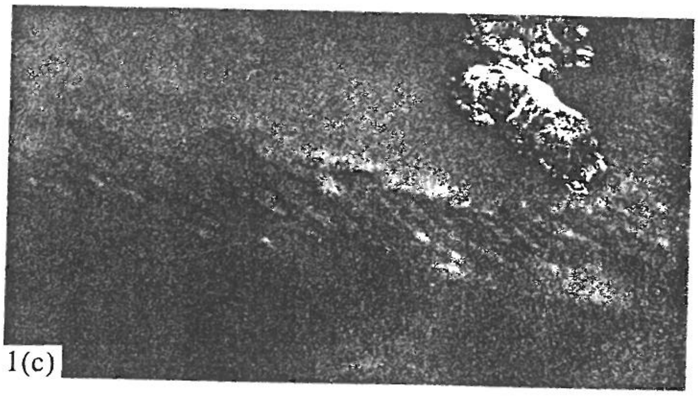

1(c)

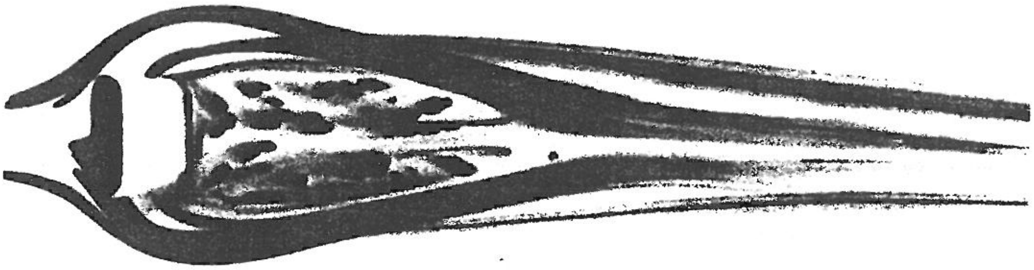

1(d)

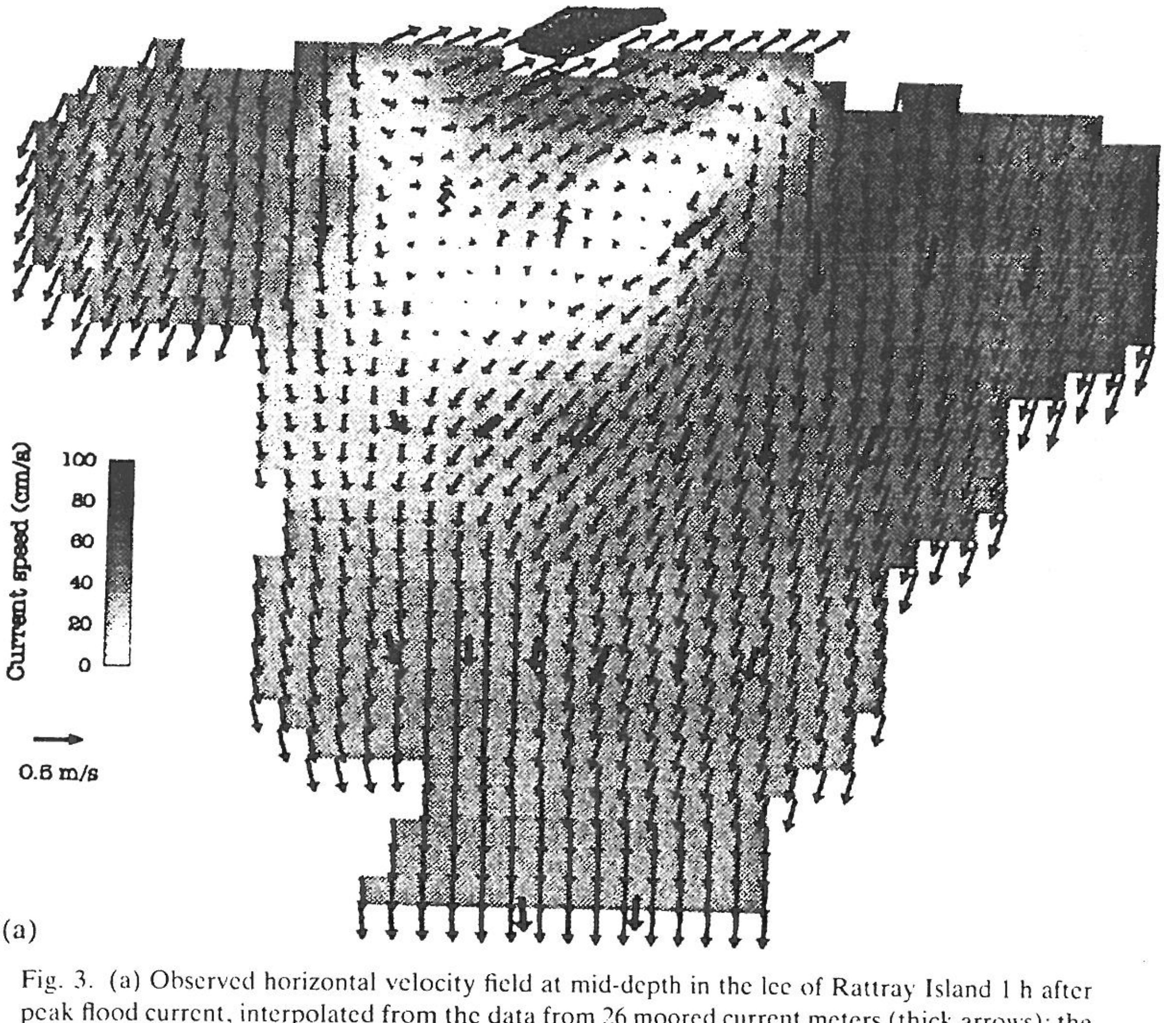

3(a)

Fig. 3. (a) Observed horizontal velocity field at mid-depth in the lee of Rattray Island 1 h after peak flood current, interpolated from the data from 26 moored current meters (thick arrows): the shading corresponds to the current speed. Predicted horizontal (arrows) and vertical (shading) velocity distribution at mid-depth in the lee of Rattray Island in (b) the absence and (c) in the presence of a free shear layer, at the same time as in (a).

(a)

(b)

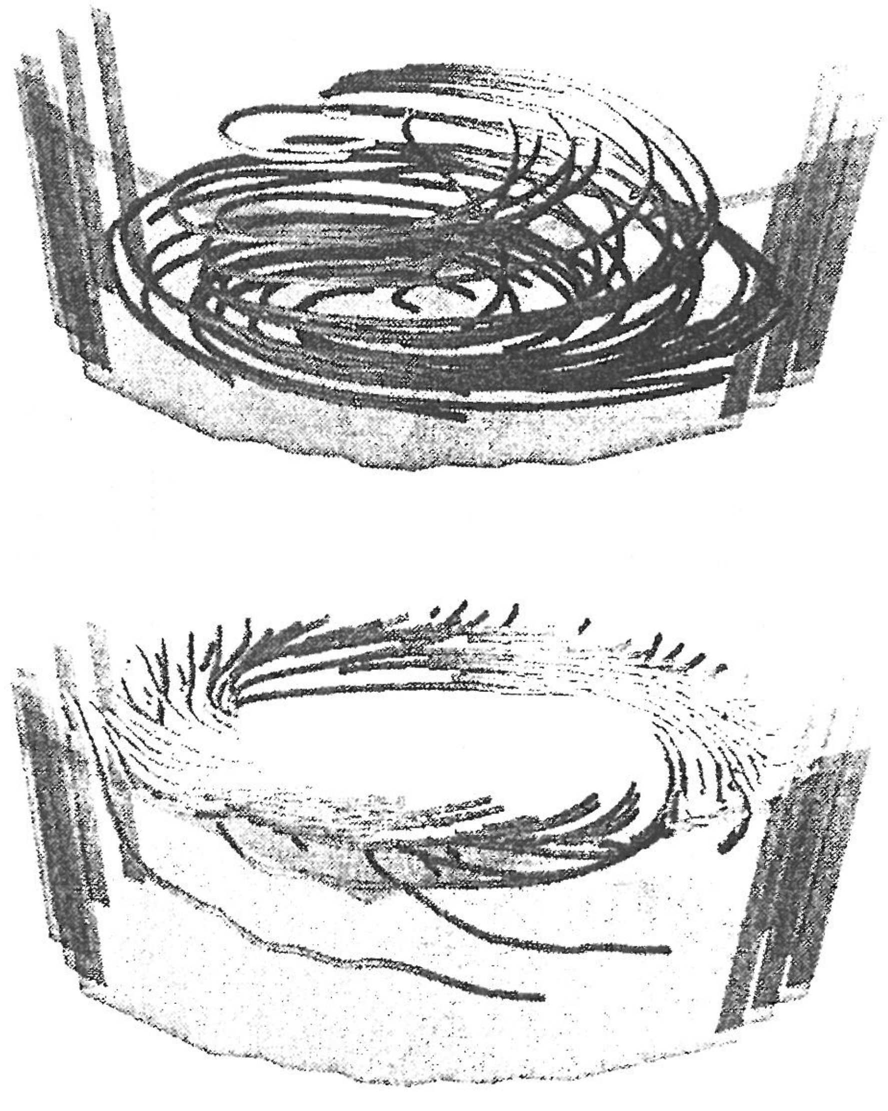

Fig. 6. Oblique views of predicted three-dimensional streamlines in a wind-forced rotating flow in a circular basin showing (a) the upwelling in the bulk of the eddy and (b) the downwelling in a very narrow zone along the edges. The basin has solid vertical walls. The graph is vertically distorted since the basin is 4000 m wide and 5 m deep. These images were produced using IBM DX programs.

predicted horizontal velocities are in close agreement with the observations from 26 moored current meters.

METHODS

Field observations

The field site was Rattray Island, Australia (Fig. 1b). The island is about 1500 m across in depths of 20–30 m. Data from 26 current meters moored in the lee of Rattray Island (Wolanski *et al.*, 1984a) are available showing details of the formation of an eddy in the lee of the island at flood tide. The maximum free stream velocity u was 0.7 m s^{-1}. Time series of aerial photographs were obtained during the formation of the eddy and were used to estimate the upwelling velocity as the time it took for fine sediment to reach the surface. These photographs demonstrated also the presence of a free shear layer shed from the separation point at the northern tip of the island. The trajectories of radar-tracked drogues were available on either side of the free shear layer. High-frequency echo-soundings were obtained along a transect crossing a free shear layer behind a small headland in shallow, well-mixed coastal waters (Wolanski, 1993).

Numerical model

The three-dimensional model of Deleersnijder *et al.* (1992) was used. This model solves numerically the fully non-linear, σ-coordinates three-dimensional equations of motion using a staggered, finite-difference, vertically implicit scheme which is based on the finite volume approach (Nihoul *et al.*, 1989). Because the waters are shallow and well-mixed, the vertical eddy diffusion coefficient K_z is taken to be

$$K_z = \alpha u_* z\,(1 - 0.6\, z/H) \tag{1}$$

where u_* is the shear velocity, H the depth, α is a constant and z the elevation above the bed. The constant α can be taken as the Karman constant ($\alpha = 0.4$) but other values are possible (Fischer *et al.*, 1979). The horizontal eddy diffusion coefficient is set equal to 2.5 $m^2\,s^{-1}$ following field observations at Rattray Island, Australia (Wolanski *et al.*, 1984a). The numerical mesh comprised 43 × 61 grid lines on the horizontal and five levels in the vertical direction. The horizontal mesh size is 200 m and the time step is 5 s.

Laboratory studies

Experiments were performed with a tilting flume, 19 m long and 0.5 m wide (Fig. 2). The bottom was smooth. A rectangular island with curved edges was installed at the middle. Five islands were modeled. Their width L (the dimension facing the current) varied between 0.01 and 0.145 m. The free stream velocity (u) was adjusted to be horizontally homogeneous within less than 1% error in velocity, except for the boundary layer at the side wall. The experiments were carried out in a range of u values between 0.02 and 0.2 m s^{-1}. The Reynolds number (Batchelor, 1967),

$$R_e = u\, L/\nu \tag{2}$$

where ν is the kinematic viscosity, of the experiments thus varied between 1000 and

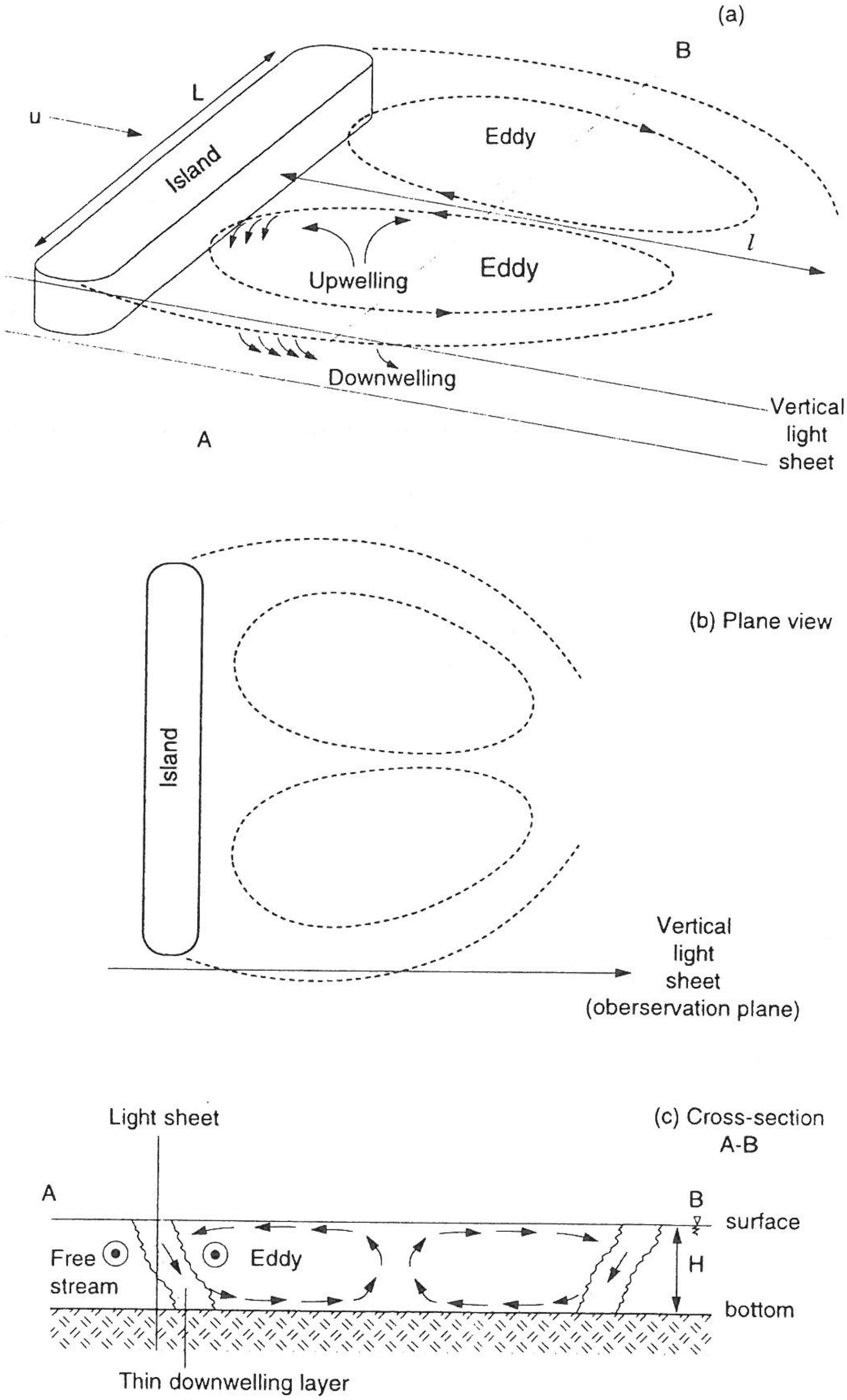

Fig. 2. (a) Oblique, (b) plane view and (c) cross-sectional sketch of the three-dimensional circulation in the laboratory island wake.

30,000. Water depth H was typically between 0.005 and 0.02 m. For shallow water flows dominated by bottom friction, some characteristics of motions, such as laminar or turbulent flows, depend on local conditions rather than on the entire flow field, suggesting that the Reynolds number based on the depth ($R_{eH} = u\,H/\nu$) is the governing parameter. R_{eH} ranged from 100 to 2000, indicating that the flow varied from laminar to fully turbulent. Correspondingly, the vertical eddy viscosity (K_z) varied from the molecular viscosity of water to the value induced by turbulent motions.

Wolanski *et al.* (1984a) and Pattiaratchi *et al.* (1986) suggested that the island wake dynamics are controlled by the island wake parameter,

$$P = (u\,L/K_z)\,(H/L)^2 \tag{3}$$

The value of K_z was calculated from empirical formulae of the bottom friction stress (τ):

$$\tau/\rho = C_D u^2 \approx K_z \partial u/\partial z \approx K_z u/H \tag{4}$$

where ρ is the density and C_D a friction coefficient. Inserting equation (4) in (3),

$$P = H/C_D\,L \tag{5}$$

where, over a smooth bed (Schlichting, 1979),

$$\begin{aligned} C_D &= 6/R_{eH} && \text{for } R_{eH} < 100 \\ C_D &= 8 \times 10^{-7} R_{eH}^{\;1.42} && \text{for } 700 < R_{eH} < 800 \\ (C_D)^{-1/2} &= 4.06\,\log_{10}(R_{eH}\sqrt{C_D}) && \text{for } R_{eH} > 800 \end{aligned} \tag{6}$$

In the present experiments, P varied between 0.3 and 120.

The eddies behind the island were visualized using dye (Fig. 1d). Styrofoam floats were photographed to obtain the surface velocity distribution. The flow direction near the bottom was measured from the displacement of a front of dissolved dye. The vertical velocity distribution along the edge of the wake region was measured using traces of aluminium particles 10^{-3} mm in diameter illuminated by a vertical light sheet and viewed from the side (Fig. 2).

RESULTS

Field results

An eddy was clearly visible in aerial photographs (Fig. 1b) and in the current meter data (Fig. 3a). Water was not stagnant in this eddy, indeed $v/u \approx 0.5$, where v is the characteristic peak velocity in the eddy and u the free stream velocity.

The aerial photographs (Fig. 1c) reveal that bottom mud can reach the surface within 1–2 h in the eddy in 20 m depth; from there the mud spirals out from the center as a result of the circular motions in the eddy and the radial velocity driven by the upwelled water reaches the surface (Fig. 1b). From the time it takes for the mud to reach the surface in an eddy, it is possible to estimate that the upwelling velocity $w_{up} \approx 0.002$–0.004 m s^{-1}.

Observations on aggregations of coral eggs at the edges of topographically shed eddies in shallow, well-mixed waters suggest that the edges of the eddies are zones of downwelling with a maximum downwelling velocity $w_{down} \approx 0.01$ m s^{-1} (Wolanski and Hamner, 1988).

The trajectories of radar-tracked drogues suggest negligible mixing between water inside and outside the eddy (Wolanski *et al.*, 1984a), these two water masses being separated by a thin free shear layer (Fig. 1c). Wolanski (1993, 1994) reported field observations of a free shear layer behind a small headland in shallow ($H < 20$ m) well-mixed coastal waters. This layer was found to be a vertical curtain of very intense three-dimensional turbulence extending from the top to bottom of the water column.

Comparison between eddies in the field and in the laboratory

The laboratories eddies resembled those shed by islands in coastal waters. Firstly, both are characterized by $H/W \ll 1$. Secondly, the laboratory eddies were visually similar to those shown in aerial and satellite photographs of Maxwell (1968), Wolanski *et al.* (1984a,b); Wolanski (1994) and Ingram and Chu (1987). The transition from no eddy to stable eddy and from stable eddy to eddy shedding occurred at the same values of P in the field and in the laboratory. Indeed, both in the field (Pattiaratchi *et al.*, 1987; Ingram and Chu, 1987; Wolanski, 1994) and in the laboratory (Fig. 4), no eddies were found for $P < 1$; for $P < 8$, stable eddies were present; eddy shedding occurred for $P > 8$.

The laboratory eddy (Fig. 1d) was geometrically similar to that at Rattray Island (i.e. $l/L \approx 2$, where l is the length of the eddy) when $P = 3.6$. In that case $v/u \approx 0.3$ in the laboratory. This compares favorably with the observation that $v/u \approx 0.5$ at Rattray Island.

In the laboratory (Fig. 2) a strong secondary circulation with an upwelling occurring in

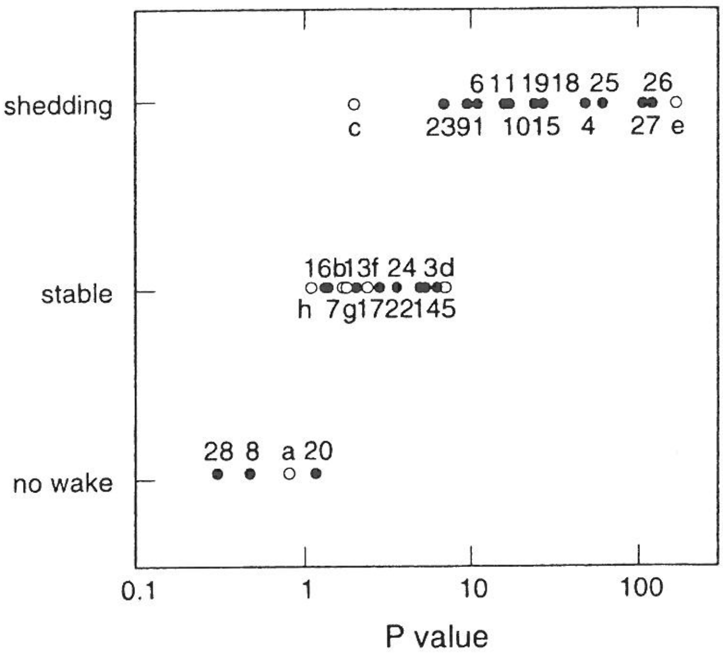

Fig. 4. The influence of the island wake parameter in determining eddy formation. The letters refer to field observations by Pattiaratchi *et al.* (1987) at Lundy Island (a–c: $H = 40$ m, $L = 4815$ m, $u \approx 0.25$–0.6 m s^{-1}), Tusker Rock (d: $H = 12$ m, $L = 100$ m, $u \approx 0.5$ m s^{-1}), Grassholm Island (e: $H = 50$ m, $L = 2.5$ m, $u \approx 2.5$ m s^{-1}), Portland Bill (f,g: $H = 30$ m, $L = 7400$ m, $u \approx 1.5$–2.0 m s^{-1}) and Porthcawl (h: $H = 2$ m, $L = 185$ m, $u \approx 0.5$ m s^{-1}). The numbers refer to the laboratory experiments.

the bulk of the eddy was found. A thin downwelling zone was observed occurring all along the edges of the eddy along the solid boundaries and also along the separation streamlines. When $P \approx 3.6$ (Fig. 5),

$$w_{down}/u \approx 0.05 \quad (7)$$

where w_{down} is the downward velocity in the thin downwelling region on the eddy side of the separation streamline. In the laboratory, the ratio w_{down}/u increases with increasing values of P, being equal to approximately 0.02 for $P = 2.0$, 0.04 for $P = 3.6$ and 0.1 for $P = 6.7$. At higher values of P the flow started to meander and reliable measurements of w became impossible; at even higher values of P, eddy shedding occurred. The upward velocity w_{up} in the bulk of the eddy was much smaller than w_{down}, typically $w_{up} \approx 0.1$–$0.3\ w_{down}$, because the upwelling zone was correspondingly larger than the downwelling zone.

This analytical model predicts that at Rattray Island where $u = 0.7$ m s^{-1}, $w_{up} \approx 0.01$–0.003 m s^{-1}, or 10–30 m h^{-1}, a result in agreement with the field observations, and $w_{down} \approx 0.01$ m s^{-1}, a result also in agreement with observations.

These shallow water eddies are quite different from those found in two-dimensional (depth-independent; Batchelor, 1967) laboratory experiments where the aspect ratio $H/L \gg 1$; in these laboratory studies, eddy water is nearly stagnant, i.e. $v/u \ll 1$ (typically $v/u = 0.01$). Similar results are obtained from depth-independent two-dimensional models (Keller and Niewstadt, 1973). Thus, the aspect ratio H/L plays a critical role; when $H/L \ll 1$, v/u is ten times larger than when $H/L \gg 1$.

These findings suggest that bottom friction is a controlling parameter in eddies in

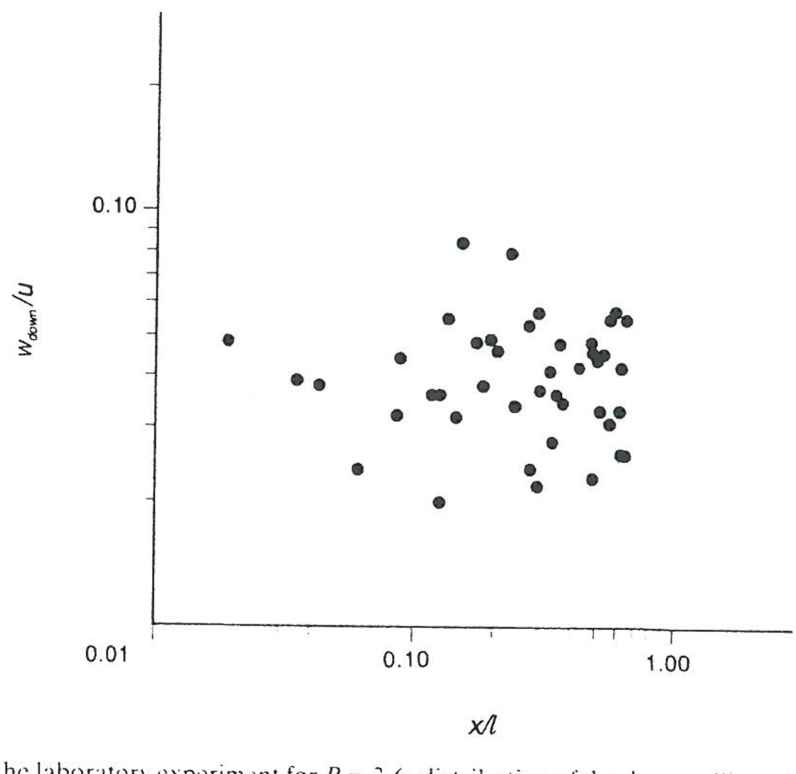

Fig. 5. For the laboratory experiment for $P = 3.6$, distribution of the downwelling velocity w_{down}, non-dimensionalized against the free stream velocity u, with distance x downstream, x is non-dimensionalized against the eddy length l.

shallow coastal waters, in the present experiments and in a Hele-Shaw cell (Von Riegels, 1938).

Numerical results

The three-dimensional model was used to simulate the circulation in a circular basin 5000 m in diameter and 5 m deep, with a flat bottom and vertical solid edges. The mesh size was 200 m. The domain was forced by a circular wind so as to generate quasi-solid body rotation, with zero horizontal velocity at the center increasing to 0.3 m s^{-1} near the edges. Friction was calculated assuming a roughness height of 0.002 m. The model successfully predicted at steady state an upwelling in the bulk of the eddy (Fig. 6a) and a downwelling in a narrow zone along the outer boundaries (Fig. 6b).

The model was applied then to the case of Rattray Island. The mesh size was 200 m and the bottom roughness height 0.002 m. The model was able to reproduce well the horizontal currents as well as an upwelling in the eddy center; however, it was unable to reproduce the downwelling along the separation streamlines (Fig. 3b). The model predictions were not changed when the mesh size was halved (not shown). Thus, the absence of a predicted downwelling along the edge of the eddy was not due to the grid being too coarse, but instead suggested that the model lacked an important physical process.

It is proposed that this process is the parameterization of the free shear layer along the separation streamline. Laboratory studies reveal that, in the free shear layer, the horizontal and vertical variations of all the components of velocity contribute to the production of turbulence. This is in contrast with the rest of the flow where turbulence is mainly generated by the vertical shearing of the horizontal velocity (Nihoul and Djenidi, 1987). The thickness of the free shear layer behind a rocky headland can be very small (2–20 m), which is sub-grid scale (Wolanski, 1993), and thus needs explicit parameterization. The numerical model was modified to explicitly parameterize the presence of a free shear layer. The free shear layer was positioned at the grid points where maximum vorticity was calculated: at these points a change of the parameter α in equation (1) was forced so that in regions of high turbulence $\alpha = 1$. This value is unknown and arbitrary, provided the vertical viscosity is not larger than the horizontal viscosity. With these modifications the model predicted a horizontal velocity distribution (Fig. 3c) in pleasing agreement with observations (Fig. 3a). The model also predicted (Fig. 3c) an upwelling occupying the bulk of the eddies, and a downwelling occurring along the free shear layers. These predictions agree with the observations. The model was unable to reproduce a downwelling if the free shear layer was parameterized by simply varying the local value of the horizontal eddy diffusion coefficient (not shown).

Depth-averaged two-dimensional numerical models of island/headland wakes in shallow coastal waters are unable to reproduce meandering and Karman vortex street at high values of P for unsteady tidal flows (Davies *et al.*, 1995), although meandering and shedding do occur in nature (Wolanski *et al.*, 1984b; Pattiaratchi *et al.*, 1987; Bowman, 1986; Wolanski, 1994). The reason for this may be that these models excessively diffuse headland-shed vorticity into the eddy, through numerical diffusion and eddy diffusion. These models cannot calculate the instability of the free shear layer, since this is a sub-grid scale phenomenon. In the simpler case of a steady far-field flow, these models appear able to predict the formation of a Karman vortex street if they are started for highly viscous fluids and the viscosity is slowly decreased in time (Dietrich *et al.*, 1994), a somewhat unrealistic assumption in the presence of a tidal current. To remedy this shortcoming, models may need much smaller grid scales (e.g. see Keller and Niewstadt, 1973) or, more simply as suggested here, an explicit parameterization of free-shear layer dynamics.

INTERNAL CIRCULATION IN EDDIES IN SHALLOW WATERS

There are fundamental differences between the internal dynamics of eddies in shallow, coastal waters according to whether they are jet-generated, or in a close basin or shed in the lee of an island or headland. Jet-generated eddies (Fig. 7a) comprise a core made of a rotational vortex where $v \propto r$, where r is the radius, surrounded by a pressure-induced, irrotational vortex where $r \propto 1/r$ (Wolanski *et al.*, 1988; Van Senden and Imberger, 1990). An upwelling has been observed in the irrotational vortex, but no downwelling zone has been reported in field and laboratory studies. Without a free shear layer to force a downwelling, jet-generated eddies are open and 'leaky' (Fig. 7a). By contrast, a closed secondary circulation can prevail in an eddy in a shallow basin (Fig. 7b) and in the lee of an island or headland (Fig. 7c) because of the presence of, respectively, a solid lateral boundary and a free shear layer.

DISCUSSION

Detailed observations are available on the horizontal velocity field in island wakes in shallow, well-mixed coastal waters. Water is far from stagnant in such eddies, indeed $v/u \approx 0.5$, where v is the peak horizontal velocity v in the eddy and u the free stream velocity. The dynamics of such eddies are thus different from those in two-dimensional depth-independent laboratory experiments where $H/L \gg 1$, where H is the depth and L the obstacle width, and the eddy waters are nearly stagnant since $v/u \ll 1$.

Field observations on the fine sediment upwelling to the surface suggest that an upwelling prevails in the bulk of the eddy with typical velocity of about 10–20 m h^{-1}. A larger downwelling velocity occurs in a narrow band along the outer edges of the eddy.

The dynamics of island wakes in shallow coastal waters appear qualitatively similar to those in laboratory experiments where $H/L \ll 1$. In such eddies, the peak velocity v is considerable, typically $v/u \approx 0.3$. Also, both in the field and in the laboratory, the transition from no eddy to a stable eddy and from a stable eddy to eddy shedding occurs at the same value of the island wake parameter. In the laboratory, an upwelling occurs in the bulk of the eddy and a downwelling in a narrow region all along the edges of the eddy. In the laboratory the downwelling velocity is considerable, typically 5–10% of the horizontal velocity.

A coarse-scale (horizontal grid size = 200 m) three-dimensional numerical model was used to simulate eddies in a closed basin 5000 m wide and 5 m deep. The model reproduced well the laboratory data. However, when applied to island wakes, the model did not reproduce the downwelling along the edges of the eddy. To remedy this, the observations of a high vertical turbulence in the sub-grid scale free shear layer were explicitly parameterized in the model. The free shear layer was modeled as a thin vertical curtain located along the separation streamline and characterized by a high value of the vertical eddy diffusion coefficient. The model predicted horizontal currents in close agreements with observations. The model also predicted a three-dimensional secondary circulation in agreement with the field observations.

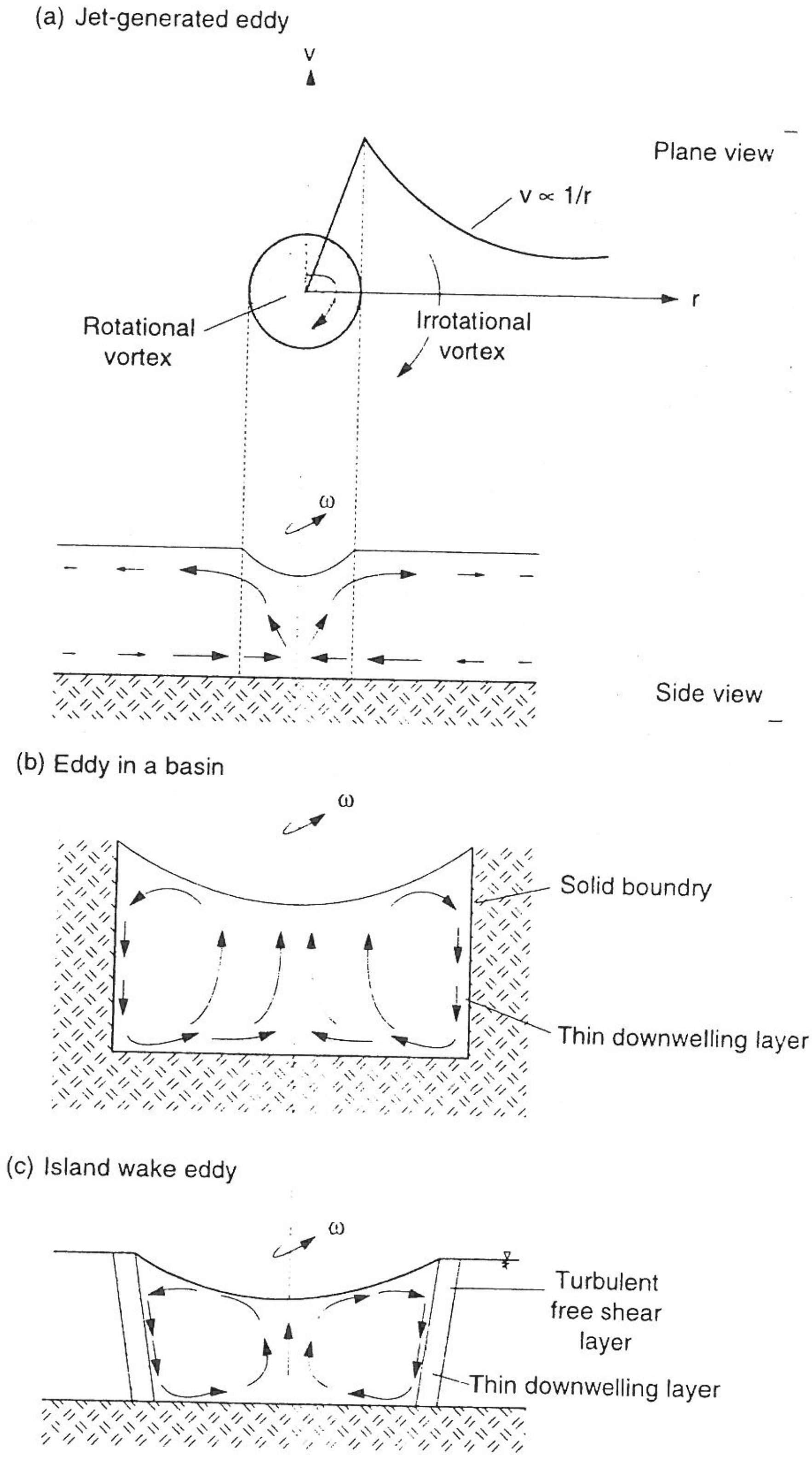

Fig. 7. Sketch of the circulation in (a) jet-generated eddies, (b) an eddy in a closed basin and (c) an island wake eddy; v is the horizontal velocity and ω the vorticity.

The parameterization of the free shear layer provides a mechanism for relatively coarse grid models to predict realistic horizontal and vertical currents near a complex topography. This parameterization may allow advection–diffusion models to realistically predict the aggregation of buoyant matter at the surface along the edge of the eddy in well-mixed waters. This secondary circulation also finds geomorphic, navigation and engineering applications as it controls the formation and movement of shoals and sand banks and even the migration of river meanders.

Free shear layers are a common occurrence and are readily visible to the naked eye; they seem to play an important role in the oceanography and the biological processes in coastal waters, yet they have been largely neglected. Detailed studies of free shear layer dynamics are warranted.

Acknowledgements—The laboratory studies were carried out at Saitama University, and the field and numerical studies at the Australian Institute of Marine Science. The authors take pleasure in thanking D. Galloway for his invaluable assistance. This study was made possible by a grant from the IBM International Foundation.

REFERENCES

Alldredge A. L. and W. H. Hamner (1980) Recurring aggregation of zooplankton by a tidal current. *Estuarine, Coastal & Shelf Science*, **10**, 31–37.

Batchelor, G. K. (1967) *An introduction to fluid dynamics*. Cambridge University Press, Cambridge, 615 pp.

Boden B. P. (1952) Natural conservation of insular plankton. *Nature*, **169**, 697–699.

Bowman K. J. (1986) The simulation of phytoplankton production on the continental shelf within von Karman vortex sheets. *Lecture Notes on Coastal & Estuarine Studies*, **17**, 107–139.

Davies P. A., J. M. Dakin and R. A. Falconer (1995) Eddy formation behind a coastal headland. *Journal of Coastal Research*, **11**, 154–167.

Deleersnijder E., A. Norro and E. Wolanski (1992) A three-dimensional model of the water circulation around an island in shallow water. *Continental Shelf Research*, **12**, 891–906.

Dietrich D. E., M. J. Bowman, C. A. Liu and A. Mestas-Nunez (1994) *Numerical studies of small island wakes*. Technical Report 94-1, Mississippi State University, Center for Air Sea Technology, Stennis Space Center, Mississippi, 36 pp.

Falconer R. A., E. Wolanski and L. Mardapitta-Hadjipandeli (1986) Modeling tidal circulation in an island's wake. *Journal of Waterway, Port, Coastal & Ocean Engineering—ASCE*, **112**, 234–254.

Fischer H., E. List, R. Koh, J. Imberger and N. H. Brooks (1979) *Mixing in inland and coastal waters*, Academic Press, New York, 883 pp.

Franks P. J. S. (1992) Phytoplankton blooms at front: patterns, scales, and physical forcing mechanisms. *Reviews in Aquatic Sciences*, **6**(2), 121–137.

Geyer W. R. (1993) Three-dimensional tidal flow around headlands. *Journal of Geophysical Research*, **98**, 955–966.

Geyer W. R. and R. Signell (1990) Measurements of tidal flow around a headland with a shipboard acoustic Doppler current profiler. *Journal of Geophysical Research*, **95**, 3189–3197.

Hamner W. M. and I. R. Hauri (1977) Fine-scale currents in the Whitsunday Islands, Queensland, Australia: effect of tide and topography. *Australian Journal of Marine & Freshwater Research*, **28**, 333–359.

Hamner W. M. and I. Hauri (1981) Effects of island mass: water flow and plankton pattern around a reef in the Great Barrier Reef lagoon, Australia. *Limnology & Oceanography*, **26**, 1084–1102.

Heathershaw A. D. and F. D. C. Hammond (1980) Secondary circulation near sand banks and in coastal embayments. *Deutsche Hydrographische Zeitschrift*, **33**, 135–151.

Ingram R. G. and V. C. Chu (1987) Flow around islands in Rupert Bay: an investigation of the bottom friction effect. *Journal of Geophysical Research*, **92**, 14521–14533.

Keller H. B. and F. Niewstadt (1973) Viscous flow past circular cylinders. *Computers & Fluids*, **1**, 59–71.

Kikkawa H., S. Ikeda and A. Kitagawa (1976) Flow and bed topography in curved open channels. *Journal of the Hydraulic Division—ASCE*, **102**, 1327–1342.

Kingsford M. J., E. Wolanski and J. H. Choat (1991) Influence of tidally induced fronts and Langmuir circulations on distribution and movements of presettlement fishes around a coral reef. *Marine Biology*, **109**, 167–180.

Maxwell W. G. H. (1968) *Atlas of the Great Barrier Reef*. Elsevier, Amsterdam, 258 pp.

Nihoul J. C. J. and S. Djenidi (1987) Perspective in three-dimensional modelling of the marine system. In *Three-dimensional models of marine and estuarine dynamics*, J. C. J. Nihoul and B. M. Jamart, editors. Elsevier Oceanographic Series, Amsterdam, pp. 1–34.

Nihoul J. C. J., E. Deleersnijder and S. Djenidi (1989) Modelling the general circulation of shelf seas by 3D k-ε models. *Earth-Science Reviews*, **26**, 163–189.

Oliver J. K., B. King, B. Willis, R. Babcock and E. Wolanski (1992) Dispersal of coral larvae from a lagoonal reef. II. Comparison between model predictions and observed concentrations. *Continental Shelf Research*, **12**, 873–889.

Pattiaratchi C., A. James and M. Collins (1987) Island wakes and headland eddies: a comparison between remotely sensed data and laboratory experiments. *Journal of Geophysical Research*, **92**, 783–794.

Pingree R. D. and L. Maddock (1979) The tidal physics of headland flows and offshore tidal bank formation. *Marine Geology*, **32**, 269–289.

Schlichting H. (1979) *Boundary layer theory*, 2nd Edition. McGraw Hill, New York, 817 pp.

Signell R. P. and W. R. Geyer (1991) Transient eddy formation around headlands. *Journal of Geophysical Research*, **96**, 2561–2575.

Simpson J. H., P. Tett, M. Argote-Espinoza, A. Edwards, K. Jones and G. Savidge (1982) Mixing and phytoplankton growth around an island in a stratified sea. *Continental Shelf Research*, **1**, 15–31.

St. John M. A. and S. Pond (1992) Tidal plume generation around a promontory: effects on nutrient concentrations and primary productivity. *Continental Shelf Research*, **12**, 339–354.

Uda M. and M. Ishino (1958) Enrichment pattern resulting from eddy systems in relation to fishing grounds. *Journal of Tokyo University of Fisheries*, **44**, 105–129.

Van Senden D. C. and J. Imberger (1990) Effects of initial conditions and Ekman suction on tidal outflows from inlets. *Journal of Geophysical Research*, **95**, 13373–13391.

Von Riegels F. (1938) Zur kritik des Hele-Shaw Versuchs. *Zeitschrift fur Angewandte Mathematik & Mechanik*, **18**, 95–106 (in German).

Wolanski E. (1993) Facts and numerical artefacts in modeling the dispersal of crown-of-thorn starfish larvae in the Great Barrier Reef. *Australian Journal of Marine & Freshwater Research*, **44**, 427–436.

Wolanski E. (1994) *Physical oceanographic processes of the Great Barrier Reef*, CRC Press, Boca Raton, FL, 194 pp.

Wolanski E. and W. M. Hamner (1988) Topographically controlled fronts in the ocean and their biological influence. *Science*, **241**, 177–181.

Wolanski E., J. Imberger and M. L. Heron (1984a) Island wakes in shallow coastal waters. *Journal of Geophysical Research*, **89**, 553–569.

Wolanski E., G. L. Pickard and D. L. B. Jupp (1984b) River plumes, coral reefs and mixing in the Gulf of Papua and the northern Great Barrier Reef. *Estuarine, Coastal & Shelf Science*, **18**, 291–314.

Wolanski E., E. Drew, K. M. Abel and J. O'Brien (1988) Tidal jets, nutrient upwelling and their influence on the productivity of the alga Halimeda in the Ribbon Reefs, Great Barrier Reef. *Estuarine, Coastal & Shelf Science*, **26**, 169–201.

Wolanski E., D. Burrage and B. King (1989) Trapping and dispersion of coral eggs around Bowden Reef, following mass coral spawning. *Continental Shelf Research*, **9**, 479–496.